Supporting Information

Catalytic Self-Assembly of Quantum Dot-Based MicroRNA Nanosensor Directed by Toehold-Mediated Strand Displacement Cascade

Fei Ma,‡ Qian Zhang,‡ Chun-yang Zhang*

College of Chemistry, Chemical Engineering and Materials Science, Key Laboratory of Molecular and Nano Probes, Ministry of Education, Collaborative Innovation Center of Functionalized Probes for Chemical Imaging in Universities of Shandong, Shandong Provincial Key Laboratory of Clean Production of Fine Chemicals, Shandong Normal University, Jinan 250014, China.

* Corresponding Authors: E-mail: cyzhang@sdnu.edu.cn

‡ These authors contributed equally to this work.

Table of Contents

1. EXPERIMENTAL SECTION

Materials. All oligonucleotides (Table S1) were purchased from TaKaRa Biotechnology Co., Ltd. (Dalian, China). Deoxynucleotide (dNTP) solution mix, Luna® universal qPCR master mix, M-MuLV reverse transcriptase and 10 × M-MuLV reverse transcriptase reaction buffer (500 mM Tris-HCl, 750 mM KCl, 30 mM $MgCl_2$, 100 mM DTT, pH 8.3) were obtained from New England Biolabs (Beverly, MA, USA). Diethylpyrocarbonate (DEPC)-treated water was obtained from Sangon Biotech Co., Ltd. (Shanghai, China). Tris-EDTA buffer solution, Trizma® hydrochloride (Tris-HCl), sodium chloride (NaCl), potassium chloride (KCl), magnesium chloride ($MgCl_2$), ammonium sulfate ($(NH4)_2SO_4$), bovine serum albumin (BSA), glycine-potassium hydroxide (KOH), glucose oxidase, D-glucose, catalase and trolox were purchased from Sigma-Aldrich Company (St. Louis, MO, USA). SYBR Gold was obtained from Life Technologies (Carlsbad, CA, USA). The streptavidin-conjugated 605QDs, Lipofectamine™ 3000 transfection reagent and Opti-MEM® I reduced-serum medium were purchased from Thermo Fisher Scientific (Massachusetts, USA). The miRNeasy RNA isolation kit was obtained from Qiagen (Valencia, CA, USA). Cell lines were obtained from cell bank of Chinese academy of sciences (Shanghai, China). The peripheral blood samples of nonsmall cell lung cancer (NSCLC) patients and healthy persons were obtained from the Affiliated Hospital of Guangdong Medical University (Zhenjiang, Guangdong, China), and the experiments were approved by the ethics committee of the Affiliated Hospital of Guangdong Medical University. Ultrapure water obtained from a Millipore filtration system was used throughout all experiments.

Table S1. Sequences of the Oligonucleotides[a]

note	sequence (5′ - 3′)
miR-21	UAG CUU AUC AGA CUG AUG UUG A
M-miR-21	UAG GUU AUC AGA CUG AUG UUG A
miR-155	UUA AUG CUA AUC GUG AUA GGG GU
let-7a	UGA GGU AGU AGG UUG UAU AGU U
let-7b	UGA GGU AGU AGG UUG UGU GGU U
let-7c	UGA GGU AGU AGG UUG UAU GGU U
Cy5-labeled signal probe	Cy5-T*C*A* ACA TC A GTC TGA TAA GCT AGA TGT TGA AAC CTA GCT AGC TTA TCA G*A*C *T
biotin-labeled capture probe	A*T*A* AGC TAG CTA GGT TTC AAC ATC TAG CTT ATC AGA CCG ATG TTG AAA CCT *A*G*C-biotin
RT primer	GTC GTA TCC AGT GCA GGG TCC GAG GTA TTC GCA CTG GAT ACG ACT CAA CA
forward primer	GCC CGC TAG CTT ATC AGA CTG ATG
reverse primer	GTG CAG GGT CCG AGG T

[a]The asterisk indicates the phosphorothioate modification.

Preparation of capture probe and signal probe with hairpin structure. The capture probe and signal probe were diluted to 2 μM in 1× reaction buffer (20 mM Tris-HCl, 140 mM NaCl, 5 mM KCl, pH 7.5), and then incubated at 95 °C for 5 min, followed by slowly cooling to room temperature over 30 min to make the probes fold into hairpin structures. The obtained hairpin

probes were stored at -20 °C prior to use.

Self-assembly of the 605QD/DNA/Cy5 nanostructure. The 60 μL of solution containing different-concentration miR-21, 5.4 μL of capature probes (2 μM), 5.4 μL of signal probes (2 μM), 6 μL of 10× reaction buffer (200 mM Tris-HCl, 1.4 M NaCl, 50 mM KCl, pH 7.5), 3 μL of 1 mg/mL BSA were incubated at 37 °C for 3 h, following by the addition of 6 μL of 605QDs (50 nM) and further incubation at 37 °C for 10 min to form the 605QD/DNA/Cy5 nanostructures. To assure the reaction time as accurate as possible in Figure 1E, the QD incubation time is reduced to 5 min before measurement.

Gel electrophoresis. To verify the assembly of capture probe/signal probe duplex, the reaction products were analyzed by 12% nondenaturating polyacrylamide gel electrophoresis (PAGE) analysis in 1× TBE (9 mM Tris−HCl, pH 7.9, 9 mM boric acid, 0.2 mM ethylenediaminetetraacetic acid, EDTA) at a 120 V constant voltage for 35 min at room temperature. To verify the assembly of the 605QD/DNA/Cy5 nanostructures, the products were analyzed by 1% agarose gel electrophoresis in 1× TAE (40 mM Tris-acetic acid, 2 mM EDTA, pH 8.0) at 110 V constant voltages for 80 min at room temperature. After electrophoresis, the gel was analyzed by a ChemiDoc™ MP Imaging System (Bio-Rad, Hercules, CA, USA).

Ensemble fluorescence measurement. Fluorescence emission spectra of the 605QD and Cy5 were measured by a Hitachi F-7000 fluorescence spectrophotometer (Tokyo, Japan) equipped with a xenon lamp as the excitation source. The spectra were recorded in the range from 550 to 750 nm

at an excitation wavelength of 488 nm. The excitation and emission slits were set for 5.0 and 5.0 nm, respectively.

Fluorescence lifetime measurement. Fluorescence lifetime measurements were performed using the time correlated single photon counting methods (TCSPC) on the FLS-1000 fluorescence spectrometer (Edinburgh Instruments Ltd., Livingston, United Kingdom). The decay curves were mono- to tetra- exponentially fitted using reconvolution fit analysis with following equation included in FLS 1000 software. The fitting formula is

$$\text{Fit} = \text{A} + \text{Fit} = \text{A} + B_1 e^{(-t/\tau_1)} + B_2 e^{(-t/\tau_2)} + B_3 e^{(-t/\tau_3)} + B_4 e^{(-t/\tau_4)}$$

where t is time, A is a constant background, B_1, B_2, B_3, and B_4 are fractional intensities, τ_1, τ_2, τ_3, and τ_4 are fluorescence lifetimes. The amplitude-weighted average fluorescence lifetime $<\tau>$ is calculated from following equation:

$$<\tau> = \frac{B_1\tau_1^2 + B_2\tau_2^2 + B_3\tau_3^2 + B_4\tau_4^2}{B_1\tau_1 + B_2\tau_2 + B_3\tau_3 + B_4\tau_4}.$$

Calculation of Förster distance. According to our previous work,[1] the Förster distance (R_0) is calculated to be 6.94 nm (or 69.4 Å) according to the following Förster formalism:

$$R_0 = \left(\frac{9000(\ln 10)\kappa_p^2 Q_D}{N_A 128\pi^5 n_D^4} I \right)^{1/6}$$

where Q_D is the quantum yield of the 605QD donor (~ 0.6) and κ^2_p is the orientation factor (2/3 for randomly oriented dipoles); N_A is the Avogadro's number, and n_D is the refractive index of the medium (~1.4 for biomolecules in aqueous solution). I is the normalized overlap integral defined as:

$$I = \int_0^\infty PL_{D-corr}\varepsilon_A(\lambda)\lambda^4 \, \mathrm{d}\lambda$$

where PL_{D-corr} is the normalized donor emission spectrum and ε_A (λ) is the acceptor absorption spectrum (expressed as an extinction coefficient, ε_A (647) = 250,000 $cm^{-1}M^{-1}$ for Cy5).

Single-molecule detection and data analysis. Before single-molecule detection, the reaction products were diluted 25-fold with the imaging buffer (1 mg/mL glucose oxidase, 0.4% (w/v) D-glucose, 0.04% mg/mL catalase, 50 μg/mL BSA, 67 mM glycine-KOH, 1 mg/mL trolox, 2.5 mM $MgCl_2$, pH 9.4). The 10 μL of samples was directly pipetted to the coverslip for the measurment. An inverted Olympus IX71 microscope (Olympus, Japan) was used for TIRF imaging, with a 488 nm laser (Coherent, USA) being used for the excitation of 605QD. Both the 605QD and the Cy5 fluorescence signals were collected by an oil immersion 100 × objective (Olympus, Japan) and imaged onto the two halves of an Andor Ixon DU897 EMCCD camera (Andor, Belfast, UK) with an exposure time of 500 ms. The single-molecule images were processed with the Analyze Particles function in Image J (Version 1.52i, NIH, Bethesda, MD, USA) to determine the number of single Cy5 spots, and the size of particle was set at 2−10 pixels to reduce the false-positive signals generated from the noise. The Cy5 spots from an imaging region of 600 × 600 pixels were counted, and the average Cy5 number was obtained from five frames at different locations.

The qRT-PCR assay. For RT reaction of microRNA, 1 μL of 10× M-MuLV reverse transcriptase reaction buffer (500 mM Tris-HCl, 750 mM KCl, 30 mM $MgCl_2$, 100 mM DTT, pH 8.3)), 0.5 μL of dNTP Mix (10 mM), 0.5 μL of RT primer (1 μM), 0.25 μL of M-MuLV reverse transcriptase (200 U/μL), the synthetic miR-21 or the total RNA extracted from real samples (cell lines or

serum) and DEPC-treated water were mixed to a final volume of 10 μL. The RT reaction was carried out at 42 °C for 45 min and then at 70 °C for 15 min. Subsequently, 5 μL of 2× Luna® universal qPCR master mix, 0.25 μL of forward primer (10 μM), 0.25 μL of reverse primer (10 μM), 1 μL of RT product and DEPC-treated water were mixed with a final volume of 10 μL. The qRT-PCR was performed under the following conditions: 95 °C for 5 min, 50 cycles of 95 °C for 10 s and 60 °C for 30 s. The real-time fluorescence measurements were performed in a Bio-Rad CFX connect Real-Time System, and the fluorescence intensity was monitored at intervals of 30 s.

Cell culture and total RNA extraction. Human lung adenocarcinoma cell line (A549 cells), human cervical carcinoma cell line (HeLa cells) and human hepatic cell line (HL-7702 cells) were cultured in Dulbecco's modified Eagle's medium (DMEM, gibco, USA) supplemented with 10 % fetal bovine serum (FBS, gibco, USA) and 1% penicillin-streptomycin. The cells were cultured at 37 ºC in a humidified atmosphere containing 5% CO_2. The number of cells was measured by Countstar cell counter. The total RNA was extracted from cells or human blood samples using the Qiagen miRNeasy RNA isolation kit according to the manufacturer's protocol, and the concentration of total RNA was determined by the NanoDrop 2000c Spectrophotometer (Thermo Scientific, Wilmington, Delaware, USA).

Imaging of microRNA in living cells. Cells were plated in 20-mm glass-bottom cell culture dish and incubated overnight in DMEM medium containing 10% fetal bovine serum. The adherent cells were washed once with 1× PBS. Transfection assays were performed using Lipofectamine™ 3000 reagent according to the manufacturer's instructions. Briefly, 7.5 μL of Lipofectamine™

3000 were diluted in 250 μL of Opti-MEM, and 12.5 μL of capture probes-605QDs (10 μM), 6.25 μL of signal probes (20 μM) and 10 μL of P3000™ were diluted in 250 μL of Opti-MEM (Invitrogen). The Opti-MEM transfection mixtures were prepared by mixing the above solutions and incubated at room temperature for 15 min. The cells were incubated with the Opti-MEM transfection mixtures at 37 °C in a humidified incubator containing 5% CO_2. After the transfection, the cells were washed five times with 1× PBS, and the dishes were filled with fresh DMEM medium containing 10% fetal bovine serum. The cell fluorescence images were obtained on an inverted Olympus IX71 microscope (Olympus, Japan) with 10× objective.

SUPPLEMENTARY RESULTS

2. Schematic illustration of the nanosensor in the absence of target microRNA

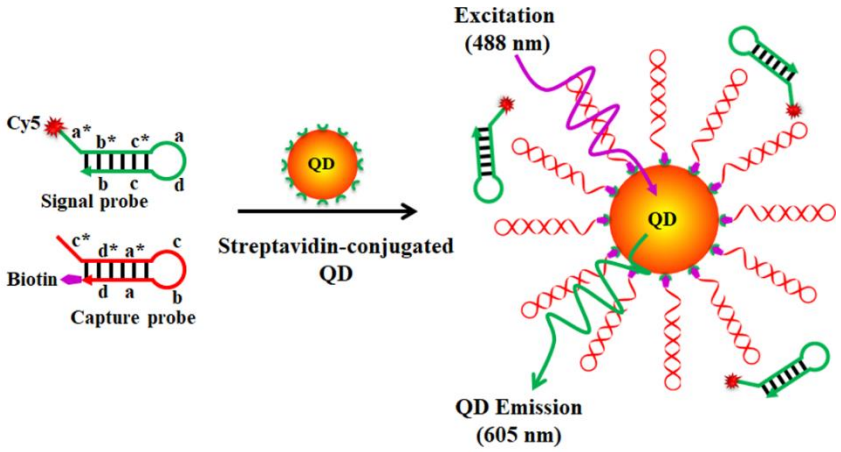

Scheme S1. Schematic illustration of the assembly of single-QD-based nanosensor in the absence of target microRNA. In the absence of target microRNA, only the capture probes are assembled on the surface of the 605QD, and no FRET occurs.

3. Normalized absorption and emission spectra of the 605QD and Cy5

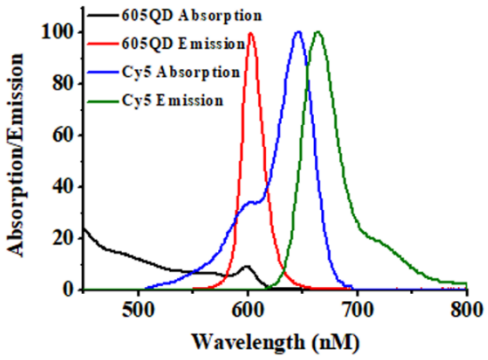

Figure S1. Normalized absorption and emission spectra of the 605QD and Cy5. Black line, absorption spectrum of the 605QD; red line, emission spectrum of the 605QD; blue line, absorption spectrum of Cy5; green line, emission spectrum of Cy5.

As shown in Figure S1, there is no spectral cross-talk between 605QD emission (Figure S1, red line) and Cy5 emission (Figure S1, green line); the large spectral overlap between 605QD emission (Figure S1, red line) and Cy5 absorption (Figure S1, blue line) enables efficient FRET from the 605QD to Cy5 under excitation of 605QD by 488-nm laser. Therefore, the 605QD and Cy5 can be used as the FRET donor and the FRET acceptor, respectively, in the proposed assay system.

4. Measurement of fluorescence emission spectra and fluorescence lifetime

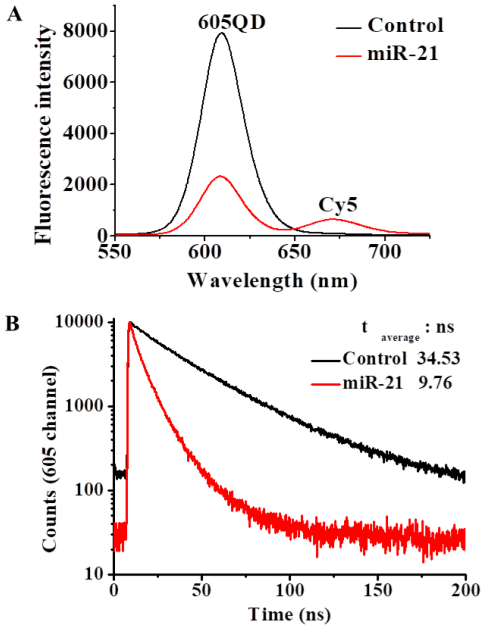

Figure S2. (A) Fluorescence emission spectra of the 605QD and Cy5 in the absence (control, black line) and presence (red line) of miR-21. Inset shows the magnified fluorescence spectra from 650 to 720 nm. (B) Fluorescence lifetime curves of the 605QD in the absence (control, black line) and presence (red line) of miR-21. The lifetime was measured in emission channel of 605 nm.

We used the ensemble fluorescence measurement to investigate the FRET resulting from the assembly of the 605QD/DNA/Cy5 nanostructure. As shown in Figure S2A, in the absence of miR-21, no Cy5-labeled signal probe is assembled on the surface of 605QD, and no Cy5 signal is detected (Figure S2A, black line). In contrast, the presence of target miR-21 can cause the decrease of 605QD emission signal accompanied by the increase of Cy5 emission signal due to the efficient FRET from the 605QD to Cy5 (Figure S2A, red line). The FRET efficiency (*E*) is calculated to be 70.73 % based on following equation:

$$E\ (\%) = (1 - F_{\text{miR-21}}/F) \times 100\%$$

where $F_{\text{miR-21}}$ is the fluorescence intensity of 605QD in the presence of miR-21 and F is fluorescence intensity of 605QD in the absence of miR-21.

As shown in Figure S2B, the average lifetime of the 605QD is 34.53 ns when target miR-21 is absent (Figure S2B, black line). The average lifetime of t is decreased to 9.76 ns with the addition of miR-21 (Figure S2B, red line), indicating the target-induced efficient FRET between the 605QD and Cy5. The FRET efficiency (*E*) is calculated to be 71.73 % based on following equation:

$$E\ (\%) = (1 - \tau_{\text{miR-21}}/\tau) \times 100\%$$

Where $\tau_{\text{miR-21}}$ is the fluorescence lifetime of 605QD in the presence of miR-21 and τ is fluorescence lifetime of 605QD in the absence of miR-21. The obtained FRET efficiency is consistent with that obtained by ensemble fluorescence measurement (Figure S2A), suggesting that the target-catalyzed assembly of QD-based nanosensor can be used for miR-21 detection.

5. Influence of reaction time and temperature upon the assay performance

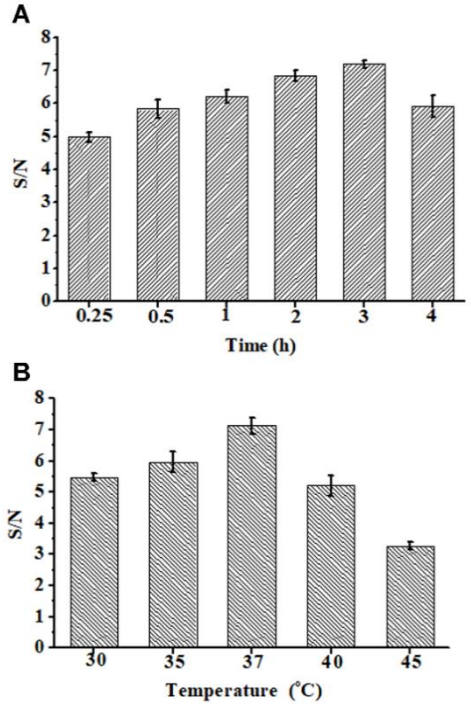

Figure S3. Variance of signal-to-noise ratio (S/N) in response to reaction time (A) and reaction temperature (B).

To achieve the best assay performance, the reaction time and reaction temperature were optimized. The signal-to-noise ratio (S/N) was used to evaluate the assay performance, which represents the ratio of Cy5 signal in the presence of miR-21 to that in the absence of miR-21. In theory, longer reaction time and higher temperature can promote the generation of a high Cy5 signal, but they may adversely induce higher background signal. As shown in Figure S3, the highest S/N is achieved at the reaction time of 3 h and reaction temperature of 37 °C. Therefore, 3 h and 37 °C are used as the optimal reaction time and the optimal reaction temperature, respectively, in the subsequent researches.

6. Influence of the Cy5-to-605QD ratio upon the assay performance

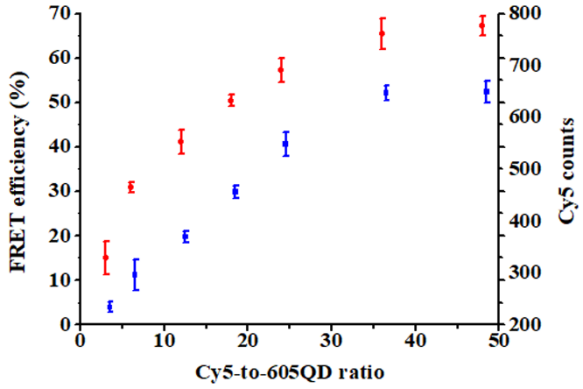

Figure S4. Variance of FRET efficiency (red color) and Cy5 fluorescence intensity (blue color) as a function of the Cy5-to-605QD ratio.

To investigate the influence of the Cy5-to-605QD ratio on the assay performance, the various concentrations of Cy5-labeled capture probe/signal probe duplexes were mixed with a fixed amount of 605QDs, and the fluorescence intensities of both the 605QDs and Cy5 at the excitation wavelength of 488 nm were measured. The FRET efficiency (E) is calculated based on following equation: E (%) = (1 – $F_{\text{miR-21}}/F$) × 100%, where $F_{\text{miR-21}}$ is the fluorescence intensity of 605QD in the presence of miR-21 and F is fluorescence intensity of 605QD in the absence of miR-21. The obtained Cy5 fluorescence intensity and FRET efficiency were plotted against the molar ratio of Cy5-labeled duplex to the 605QD. As shown in Figure S4 (red line), the FRET efficiency enhances with the increasing ratio of Cy5-labeled duplex to the 605QD from 4 to 36, and reaches a plateau beyond 36. The Cy5 counts also reach a plateau beyond the ratio of 36 (Figure S4, blue line). These results indicate the maximum loading number of the signal probe/capture probe duplexes per 605QD is 36, and obvious signal saturation is observed at high concentration of

Cy5-labeled capture probe/signal probe duplexes. Taking into account that three available biotin-binding sites after conjugation to the 605QD and there are 12 streptavidins bound on each 605QD on average,[1] our results are consistent with those obtained by biotin-4-fluorescein fluorescence quenching method.[2,3]

7. Fluorescence emission spectra in response to different-concentration target miR-21

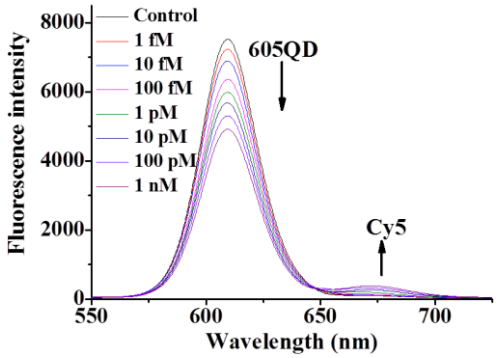

Figure S5. Fluorescence emission spectra of 605QD and Cy5 in response to increasing concentrations of miR-21 from 0 (control) to 1 nM.

8. Cy5 counts in response to high-concentration target miR-21

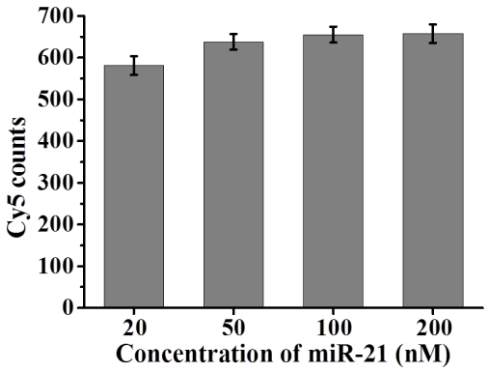

Figure S6. Measurement of Cy5 counts in response to high-concentration miR-21.

To investigate the signal saturation, Cy5 signals in response to high-concentration target miR-21

from 20 to 200 nM were measured. As shown in Figure S6, the Cy5 counts are saturated beyond 20 nM because the largest loading limit of the duplexes on QD has been reached.

9. Measurement of turnover rate

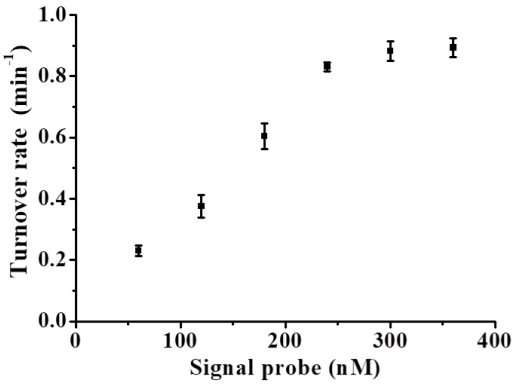

Figure S7. Variance of the turnover rate in response to different-concentration signal probes. The concentrations of miR-21 is 20 nM, and the concentrations of capture probe is 360 nM.

We further measured the turnover rate (defined as the rate of reaction divided by concentration of the catalyst) of the proposed toehold-mediated strand displacement cascade reaction by changing the signal probe concentration. As shown in Figure S7, the turnover rate enhances from 0.23 to 0.89 min^{-1} when the signal probe concentration increases from 60 to 360 nM. These results suggest that the proposed toehold-mediated strand displacement cascade reaction provides rapid and efficient signal amplification towards target miR-21.

10. The qRT-PCR measurement

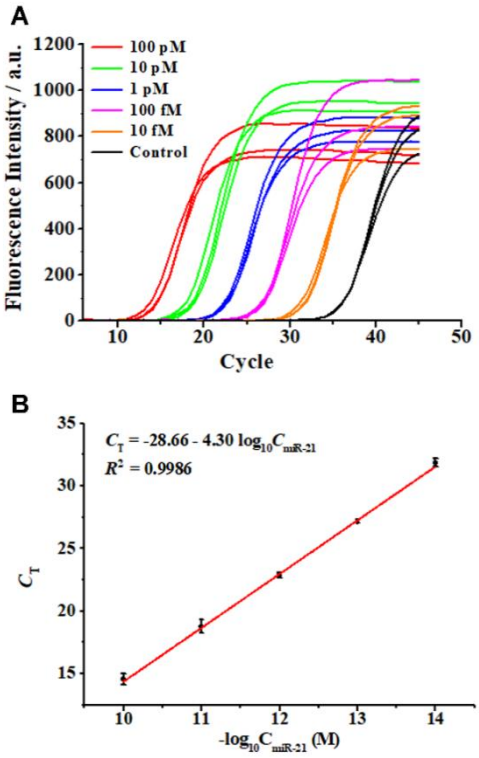

Figure S8. (A) Real-time fluorescence monitoring of the PCR amplification reaction in response to increasing concentrations of miR-21 from 0 (control) to 100 pM. (B) Linear relationship between the C_T value and the logarithm of miR-21 concentration.

The standard qRT-PCR method is used as the reference to demonstrate the accuracy of the proposed assay. After the reverse transcription reaction of target microRNA, the products were subjected to quantitative PCR analysis. The real-time fluorescence curves in response to different-concentration miR-21 are shown in Figure S8. The C_T value has a linear correlation with the logarithm of miR-21 concentration in the range from 10 fM to 100 pM, and the regression equation is C_T = -28.66 – 4.30 $\log_{10} C_{miR-21}$ with a correlation coefficient (R^2) of 0.9986, where C_{miR-21} is the concentration of target miR-21.

11. Detection sensitivity for A549 cell assay

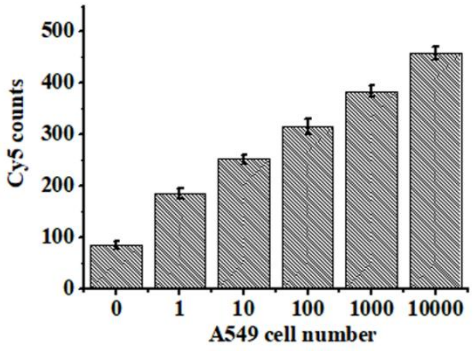

Figure S9. Variance of Cy5 counts with the A549 cell number ranging from 0 to 10000 cells.

We measured the Cy5 counts in response to RNA extracts of A549 cells with different cell numbers. As shown in Figure S9, the Cy5 counts enhance with the increasing A549 cell number from 0 to 10000 cells. Notably, the Cy5 signal of even 1 single A549 cell can be well discriminated from that of control sample without cells, indicating the proposed method can sensitively detect miR-21 at the single-cell level. The sensitivity of the proposed method is superior to the RCA-assisted electrochemiluminescent assay (100 cells)[4] and is comparable to the quadratic isothermal amplification-assisted fluorescent assay (1 cell),[5] but without the involvement of any enzyme-assisted signal amplification steps.

12. Imaging of miR-21 in A549 cells

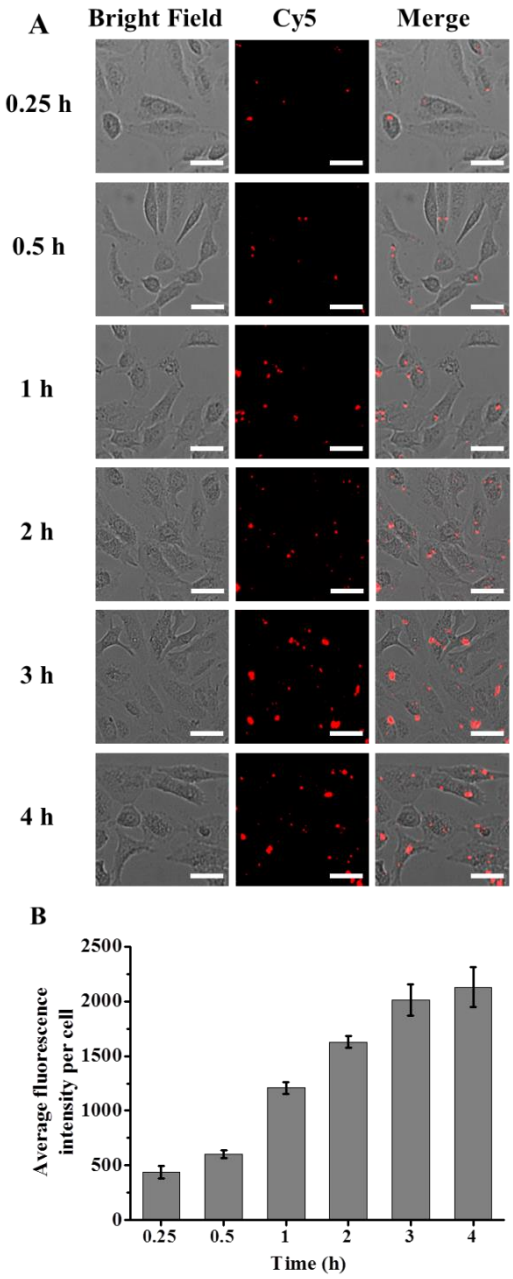

Figure S10. (A) Imaging of miR-21 in A549 cells at the indicated time. The scale bar is 100 μm. (B) Average fluorescence intensity per cell at the indicated time.

As shown in Figure S10A, distinct Cy5 signals can be detected in living A549 cells. The

average fluorescence intensity per cell enhances with the increasing incubation time from 0.25 to 3 h (Figure S10B), indicating that the proposed nanosensor can be used for imaging miR-21 in living cells in a long time scale.

13. Detection of serum circulating miR-21

Table S2. Detection of serum circulating miR-21 from NSCLC patients and healthy persons

sample	Cy5 counts	miR-21 concentration (fM, by nanosensor)	median concentration (fM)	CT value	miR-21 concentration (fM, by qRT-PCR)	median concentration (fM)
normal 1	198.86 ± 4.09	25.94 ± 3.77		29.96 ± 0.16	23.36 ± 1.93	
normal 2	197.38 ± 7.75	25.19 ±6.00		29.91 ± 0.81	25.30 ± 9.41	
normal 3	210.05 ± 4.53	38.40 ±5.82	62.59	29.06 ± 0.16	37.76 ± 3.30	65.66
normal 4	236.33 ± 3.72	95.76 ± 12.06		27.15 ± 0.18	105.43 ± 9.84	
normal 5	244.57 ± 3.68	127.66 ± 16.31		26.67 ± 0.20	136.44 ± 14.55	
patient 1	270.71 ± 2.47	316.57 ± 27.27		25.09 ± 0.06	316.35 ± 10.50	
patient 2	271.19 ± 3.27	322.76 ±37.77		24.92 ± 0.08	345.94 ± 13.87	
patient 3	262.67 ± 2.01	238.75 ± 16.61	275.32	25.57 ± 0.18	245.31 ± 23.54	286.25
patient 4	266.90 ± 3.22	277.86 ± 31.88		25.28 ± 0.23	287.60 ± 34.65	
patient 5	260.24 ± 3.77	220.64 ± 28.78		25.64 ± 0.15	236.04 ± 18.18	

14. REFERENCES

(1) Zhang, C.-Y.; Yeh, H.-C.; Kuroki, M. T.; Wang, T.-H. Single-Quantum-Dot-Based DNA Nanosensor. *Nat. Mater.* **2005**, *4*, 826-831.

(2) Lippert, L. G.; Hallock, J. T.; Dadosh, T.; Diroll, B. T.; Murray, C. B.; Goldman, Y. E. NeutrAvidin Functionalization of CdSe/CdS Quantum Nanorods and Quantification of Biotin Binding Sites using Biotin-4-Fluorescein Fluorescence Quenching. *Bioconjugate Chem.* **2016**, *27*, 562-568.

(3) Mittal, R.; Bruchez, M. P. Biotin-4-Fluorescein Based Fluorescence Quenching Assay for Determination of Biotin Binding Capacity of Streptavidin Conjugated Quantum Dots. *Bioconjugate Chem.* **2011**, *22*, 362-368.

(4) Chen, A.; Ma, S.; Zhuo, Y.; Chai, Y.; Yuan, R. In Situ Electrochemical Generation of Electrochemiluminescent Silver Naonoclusters on Target-Cycling Synchronized Rolling Circle Amplification Platform for MicroRNA Detection. *Anal. Chem.* **2016**, *88*, 3203-3210.

(5) Duan, R.; Zuo, X.; Wang, S.; Quan, X.; Chen, D.; Chen, Z.; Jiang, L.; Fan, C.; Xia, F. Lab in a Tube: Ultrasensitive Detection of MicroRNAs at the Single-Cell Level and in Breast Cancer Patients Using Quadratic Isothermal Amplification. *J. Am. Chem. Soc.* **2013**, *135*, 4604-4607.